Rechargeable batteries

Chapter 5.3

RECHARGEABLE BATTERIES
Efficient Energy Storage Devices for Wireless Electronics

P.H.L. Notten
Philips Research Eindhoven, Eindhoven University of Technology
peter.notten@philips.com

Abstract Batteries are indispensable in our present-day portable society. In order to feet the wide variety of portable and wireless electronic equipment we can nowadays rely on various battery systems, each having its own specific advantages and disadvantages. In this contribution, the basic principles of the most popular battery systems are reviewed, including Nickel–MetalHydride, Nickel–Cadmium, and Lithium–ion.

Keywords rechargeable batteries; Nickel–MetalHydride; Nickel–Cadmium; Li–ion

1. INTRODUCTION

Rechargeable batteries are energy storage devices, which are able to convert chemically stored energy into electrical energy during discharging and vice versa during recharging. The application of batteries to provide portable equipment with electrical energy has been rapidly growing during the last decades. Various types of commercially available batteries are used nowadays, varying from small button-type cells used in small-size electronics to batteries for hybrid cars and other large-scale electrical storage applications. Two classes of batteries can, in principle, be distinguished (see Table 5.3-1).

The first group is formed by the primary cells. These types of batteries can, in general, not be recharged and are therefore considered as non-rechargeable. The most popular member of this class, often applied in

Mukherjee
Hardware Technology Drivers of Ambient Intelligence

Table 5.3.1. Open-circuit potentials and energy density values for various primary (nonrechargeable) and secondary (rechargeable) batteries.

	System	Open-circuit potential (V)	Energy density*	
			Wh/kg	Wh/l
Primary Batteries	$Zn - MnO_2$	1.6	80–150	300–400
	Zn–air	1.65	300–400	800–1300
Secondary Batteries	SLA	2.1	30–40	70–80
	NiCd	1.3	35–65	100–200
	NiMH	1.3	40–90	160–310
	Li–ion	3.8	100–160	200–400

*Energy densities are strongly dependent on discharge rate.

many portable electronics, is the alkaline Zinc–Manganesedioxide ($ZnMnO_2$) cell. Another example is the Zinc–air (Zn–air) button cell, commonly used in hearing aids, although formally speaking, this system should be positioned in between a battery and a fuel cell system, as the oxygen electrode is based on the fuel cell concept of ''external'' chemical storage rather than the battery concept, relying on ''internal'' chemical storage inside the battery electrodes.

The second group is formed by the so-called secondary cells. These can be recharged once they are partly or completely discharged. During recharging, electrical energy is converted again into chemical energy by means of a charging device. It is evident that for applications, which frequently need a lot of ''portable energy,'' such as cellular telephones, laptop computers, PDA's, and electrical shavers, rechargeable batteries are preferred, not only for economical reasons but also for our convenience. This chapter will therefore focus on rechargeable batteries only.

Various types of rechargeable batteries are available and the number is still expanding. The most popular types are, at the moment, the conventional Nickel–Cadmium (NiCd) battery, the high-energy dense Nickel–MetalHydride (NiMH) battery, and the most recently developed Lithium (Li–ion) batteries. There are very large differences in the characteristics and performances between the various systems. This becomes clear when one considers, for example, the battery open-circuit voltage and the energy densities of the considered systems in Table 5.3-1 [1–3]. It is obvious that these parameters may have a different impact on the electronic design of portable equipment. It should, however, be emphasized that in order to make a proper battery choice for a particular application, one has to deal with a wide variety of battery characteristics. Many aspects should already

be considered in the very early stages of the development phase. Figure 5.3-1 gives a glimpse of the various parameters, which may be taken into account.

It is an understatement to say that application of portable energy in cordless versions of consumer electronics will become even more important in the near future than is already the case now. A further expansion into the direction of *Autonomous devices* for *Ambient Intelligence* is also foreseen. Knowledge about the performance of the various battery systems is therefore indispensable. In this contribution, we will focus on the basic electrochemical principles and characteristics of the most important systems, starting with the most popular rechargeable systems. Since Philips Research can be considered as the inventor of the NiMH battery, and since NiMH batteries has taken over the NiCd market during the last decade, we will start explaining the basic electrochemical principles of this battery type. Subsequently, the differences in concepts of NiCd and Li–ion will be described. Apart from the various concepts, some electrochemical characteristics typical for these systems will be addressed as well, including, for example, their charge and discharge performance, self-discharge, and occurring memory effects.

2. NICKEL–METALHYDRIDE BATTERIES

2.1. Basic Reactions

A schematic representation of a NiMH battery containing an AB_5-type hydride-forming electrode is shown in Figure 5.3-2 [2, 3]. The electrodes

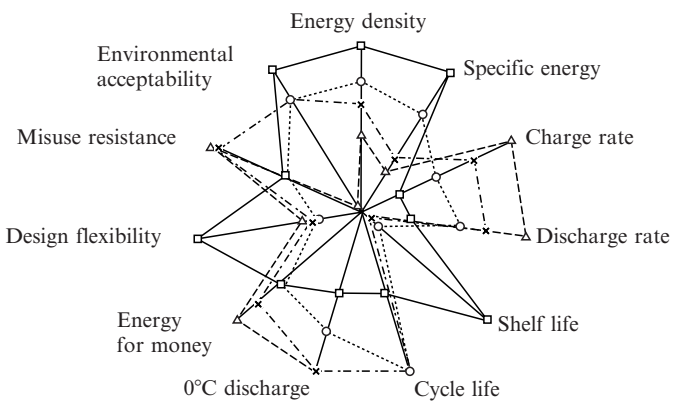

Figure 5.3-1. A wide variety of parameters characteristic for conventional and future type of batteries, which should be taken into account already in the very early development stage of new products.

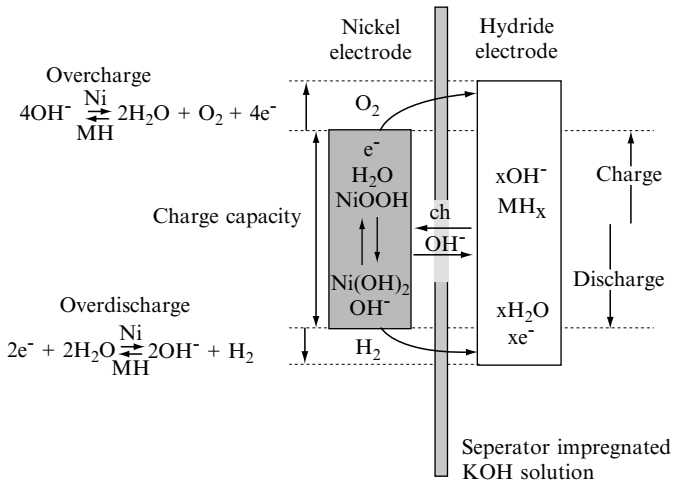

Figure 5.3-2. Schematic representation of the concept of a sealed rechargeable NiMH battery.

are electrically isolated from each other by a separator. Both separator and electrodes are impregnated with an alkaline solution, which provides for the ionic conductivity between the two electrodes. The overall electrochemical reactions, occurring at both electro during charging (ch) and discharging (d) can, in their most simplified form, be represen by:

$$\mathrm{Ni(OH)_2 + OH^- \underset{d}{\overset{ch}{\longleftrightarrow}} NiOOH + H_2O + e^-}, \tag{5.3-1}$$

$$\mathrm{AB_5 + xH_2O + xe^- \underset{d}{\overset{ch}{\longleftrightarrow}} AB_5H_x + xOH^-}. \tag{5.3-2}$$

During charging, divalent Ni^{II} is oxidized into the trivalent Ni^{III} state and water is reduced to hydrogen atoms at the metalhydride (MH) electrode, which are, subsequently, absorbed by the hydride-forming compound. The reverse reactions take place during dischar. The net effect of this reaction sequence is that hydroxyl ions in the electrolyte are transported from one electrode to the other, and hence that no electrolyte consumption takes place during current flow. For a proper functioning of a battery, it is thus essential that both electrical and ionic conductivity take place. The basic reactions are also indica in Figure 5.3-2.

In general, exponential relationships between the partial ano/ca currents and the applied electrode potential are obser under kinetic-controlled conditions, as is depicted schematically in Figure 5.3-3 (dashed curves)

[4–8]. The potential scale is given with respect to an Hg/HgO (6 N KOH) reference electrode. The equilibrium potential of the Ni-electrode under standard conditions is far more positive ($E^o_{Ni} = +439\,\text{mV}$) than that of the MH-electrode, which is found to be dependent on the plateau pressure of the hydride-forming material used (E^o_{MH} ranges between -930 and $-860\,\text{mV}$). This implies that the theoretical open-circuit potential of an NiMH battery is approximately 1.3 V, very similar to that of an NiCd battery. This makes these two different battery systems indeed very compatible, although it should already be mentioned here that small differences in performance exist between both systems.

During galvanostatic charging of the NiMH battery with a constant current, an overpotential (η) will be established at both electrodes. The magnitude of each overpotential component (η_{Ni} and η_{MH} in Figure 5.3-3) is determined by the kinetics of the charge transfer reactions. An electrochemical measure for the kinetics of a charge transfer reaction is generally considered to be the exchange current I^o, which is defined at the equilibrium

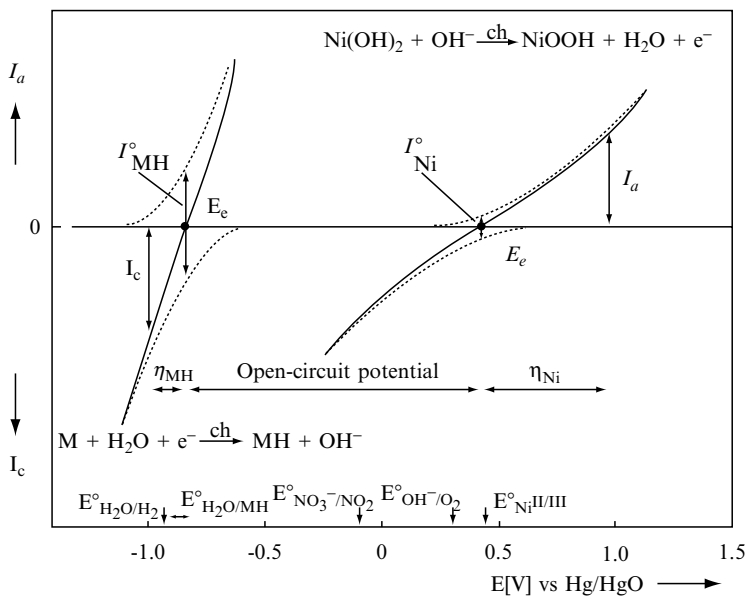

Figure 5.3-3. Schematic representation of the current-potential curves for an Ni and MH electrode (solid lines), assuming kinetically controlled charge transfer reactions. The partial anodic and cathodic reactions are indicated as dashed lines. The exchange currents (I^o) are defined at the equilibrium potentials (E_e). Potentials are given with respect to a Hg/HgO reference electrode. Besides the redox potentials (E^o) of the main electrode reactions, those of some side-reactions are also indicated.

potential, E_e, where the partial anodic current equals the partial cathodic current (see Figure 5.3-3).

In case of the Ni-electrode I^o is reported to be relatively low ($I^o_{Ni} = 10^{-7}\,\mathrm{A/cm^2}$), which implies that at a given constant anodic current, I_a, the overpotential at the Ni-electrode is relatively high (see Figure 5.3-3). In contrast, the kinetics of the MH-electrode is known to be strongly dependent on the materials composition. Assuming a highly electrocatalytic hydride-forming compound, this implies that the current-potential curves, characteristic for the MH-electrode are very steep in comparison to those for the Ni-electrode, resulting in a much smaller value for η_{MH} at the same cathodic current I_c, as is schematically shown in Figure 5.3-3. It is evident that the battery voltage under current flow is a summation of the open-circuit potential and the various overpotential components. This includes the ohmic potential drop (η_{IR}) caused by the electrical resistance of the electrolyte (R_e). The reverse processes occur during discharging, resulting in a cell voltage lower than 1.3 V. Clearly, since the potential of both electrodes may change considerably, the absolute values of these potentials cannot be directly deduced from the cell voltage. The use of a reference electrode is therefore inevitable in order to interpret the current-potential dependencies in an appropriate way.

It can be concluded that the kinetics of the charge transfer reactions can generally be described by exponential relationships, denoted as the Butler–Volmer equations. These nonlinear relationships indicate that the so-called charge transfer resistances do not have constant values but are dependent on the applied current. The Butler–Volmer relationships can simply be characterized by two parameters (i.e., the equilibrium potential E_e and the exchange current I^o). It should, however, be noted that these parameters do not have fixed values but are dependent on the concentration of the electroactive species involved in the charge transfer reactions, and thus change as a function of state-of-charge [2, 8]. This is schematically illustrated for the current-potential characteristics for the MH electrode in Figure 5.3-4.

The anodic oxidation of stored hydrogen atoms is here shown to be dependent on the hydrogen concentration at the electrode surface, whereas the reduction rate of water is independent (no water is consumed) on the state-of-charge. As a result, the complete current-potential curves (bold lines), and hence the indicated values for E_e and I^o, change significantly as a function of state-of-charge (SoC). This holds, of course, not only for the metalhydride electrode, but also for other electrodes. This makes an appropriate mathematical description of an entire battery much more complex [4–8].

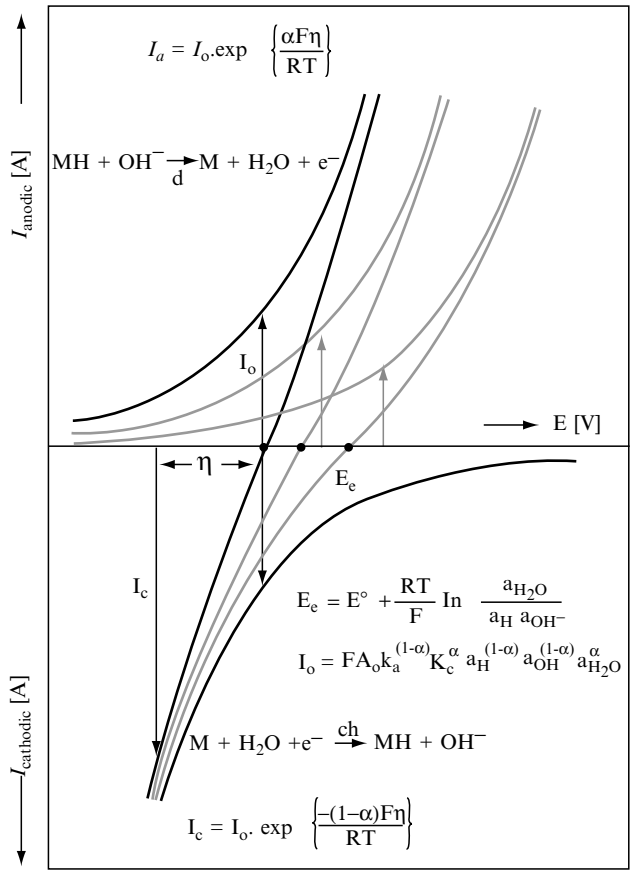

Figure 5.3-4. Schematic representation of the dependence of the partial anodic current-potential curves on the hydrogen concentration within the solid of a metalhydride electrode (i.e., at different states-of-charge). The hydride formation is state-of-charge independent. As a consequence, the overall Butler–Volmer relationships (solid lines) reveal that both the equilibrium potential (E_e) and the exchange current (I^o) change as a function of state-of-charge.

2.2. Side Reactions

2.2.1. Overcharging

To ensure the well-functioning of sealed rechargeable NiMH batteries under a wide variety of conditions, the battery is designed in such a way that the Ni electrode is the capacity-determining electrode, as is schematically indicated in Figure 5.3-2. Such a configuration forces side-reactions

to occur at the Ni electrode, both during overcharging and overdischarging, as is shown later.

During overcharging OH^- ions are oxidized at potentials more positive with respect to the standard redox potential of the OH^-/O_2 redox couple (about 0.3 V with respect to the Hg/HgO reference potential), and oxygen evolution starts at the Ni electrode, according to:

$$4OH^- \overset{\text{Ni}}{\longleftrightarrow} O_2 + 2H_2O + 4e^-. \tag{5.3-3}$$

Again, an exponential relationship between the current and potential is to be expected, as is shown in curve (a) of Figure 5.3-5 and, a more or less constant oxygen overpotential (η_{o_2}), will be established at the Ni electrode.

As a result, the partial oxygen pressure inside the sealed cell starts to rise. Advantageously, oxygen can be transported to the MH electrode, where it can be reduced at the MH/electrolyte interface in hydroxyl ions at the expense of the hydride-formation reaction (Equation 5.3-2),

$$O_2 + 2H_2O + 4e^- \overset{\text{MH}}{\longleftrightarrow} 4OH^-. \tag{5.3-4}$$

When this reduction reaction is kinetically controlled, an exponential dependence is also to be expected for this reduction reaction, as is shown in curve (b) of Figure 5.3-5.

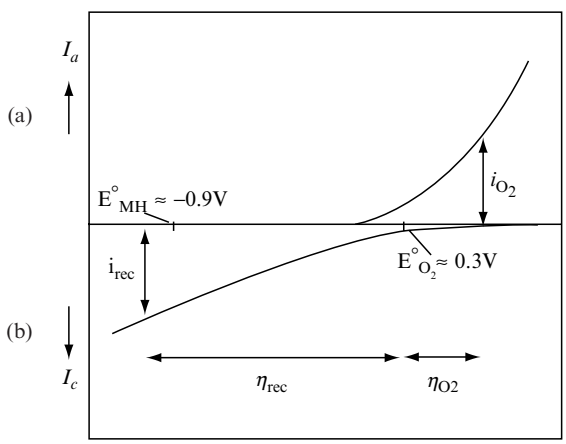

Figure 5.3-5. Schematic representation of the overcharging process inside an NiMH battery. The anodic oxygen evolution reaction (curve (a)) takes place at the Ni electrode, whereas the cathodic oxygen recombination reaction (curve (b)) occurs at the MH electrode.

It should, however, be noted that the steepness of this curve not necessarily need to be the same for both the oxygen evolution (curve (a)) and recombination reaction (curve (b)). It is even very unlikely that the kinetics of both reactions are similar as the oxidation and the reduction reactions take place at chemically different electrode surfaces, resulting in different values for the exchange current densities. All together, the above mechanism ensures that the partial oxygen pressure inside the battery can be kept very low, assuming that the recombination mechanism is functioning properly.

The parasitic oxygen evolution reaction takes place at more positive potentials than the basic Ni reaction (Eq. 5.3-1). This generally results in a rather sharp increase in the battery voltage at the end of the charging process at the point, where the overcharging process takes over. This is indeed confirmed experimentally as Figure 5.3-6 reveals.

This voltage rise is often exploited to detect the end of the charging process, although it should be noted that in general, the battery is not fully charged using this end-of-charge detection point. It is also clear from Figure 5.3-6 that the pressure inside the battery is sharply raising at the end of the charging process, around a 100% state-of-charge level, and tends to level off at higher states-of-charge. In the steady state during overcharging, the amount of oxygen evolved at the Ni electrode (represented by I_{O_2} in curve (a) of Figure 5.3-5) is equal to the amount of oxygen recombining at the MH electrode (I_{rec} in Figure 5.3-5), resulting in a

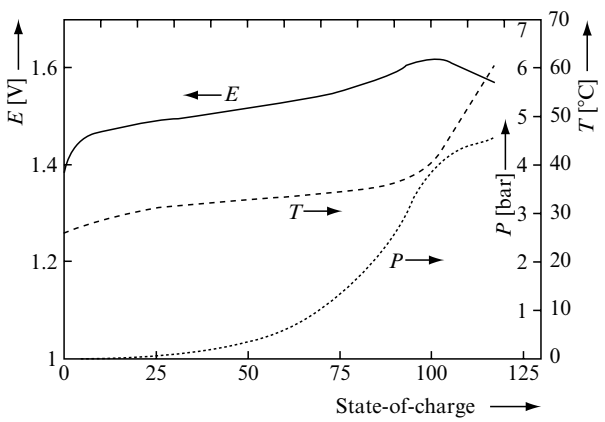

Figure 5.3-6. Development of the cell voltage (E), the internal gas pressure (P), and the cell temperature (T) as a function of state-of-charge for an NiMH battery during charging and overcharging with a high (3 A) current. The battery is then fully charged within 20 min.

constant gas pressure. Furthermore, this implies that all electrical energy supplied to the battery during overcharging is completely converted into heat. From Figure 5.3-5, it is clear that the complete battery voltage is used under these circumstances to build up the two overpotential contributions. The kinetics of this so-called recombination mechanism has been extensively studied [9].

Besides the gas pressure build-up inside a battery, the development of the battery temperature is also of considerable importance and may influence various factors in a negative sense (e.g., cycle-life). The formation of heat (W) inside a battery has been represented by

$$W = I_i \left\{ \sum_i \frac{-T\Delta S_i}{nF} + \sum_i \eta_i + I_i R_e \right\}, \tag{5}$$

where I_i is the local current flowing through the various reaction paths (i) through the battery, T the temperature, n the number of electrons involved in the overall charge transfer reaction (summation of Equations (5.3-1) and (5.3-2)), and F is the Faraday constant [5, 8]. The factors, which contribute to the evolved heat during current flow, can be easily recognized in Equation (5.3-5):

(1) The entropy change (ΔS_i) brought about by the electrochemical reactions;
(2) *The summation term is composed of the various overpotential components (η_i) and has to include the various electrochemical reactions; and*
(3) The internal battery resistance, whose contribution may be significant, especially when high currents are applied, as the heat evolution due to this effect is proportional to the square of the current.

As long as the basic electrochemical reactions (Equations (5.3-1) and (5.3-2)) proceed inside the battery, both overpotential components are relatively small. This implies that the heat contribution, resulting from the electrode reactions is limited. The temperature rise during the normal charging procedure is therefore limited, as Figure 5.3-6 reveals. However, this situation changes drastically as soon as the oxygen recombination cycle at the MH electrode starts. Since the MH electrode potential is at least 1 V more negative with respect to the standard redox potential of the OH^-/O_2 couple (see Figure 5.3-5), this implies that the established overpotential for the oxygen recombination reaction is extremely high ($>$1.2 V). Considering Equation (5.3-5), it is therefore to be expected that the heat evolved inside a battery will sharply increase as soon as the

oxygen recombination cycle starts. This is indeed in agreement with the pronounced temperature increase found during overcharging in the experiments (see Figure 5.3-6). Although the recombinati cycle moderates a considerable pressure rise inside the NiMH battery, it is essential to avoid prolonged overcharging in order to prevent a considerable temperature rise, which may negatively affect other electrode properties. In conclusion it can be said that, dependent on the kinetics of the oxygen recombination reaction (i.e., dependent on the competition between reaction in Equations (5.3-2) and (5.3-4)), the gas pressure and/or temperature of the battery will rise during overcharging. In fact the gas pressure and the temperature rise counterbalance one another when the recombination rate is very poor; the large pressure rise will be combined with a small temperature increase. On the other hand when the recombination rate is excellent, the internal pressure will be limited, while the temperature increase will be rather pronounced. Under extreme charging conditions, both effects do have a negative influence on the battery performance. It should, however, be emphasized that an exorbitant pressure rise may be fatal for the battery performance once the safety vent, with which rechargeable batteries are always equipped, has been opened. The reason for this is that during venting not only the surplus of gases, but simultaneously a significant amount of electrolyte is also released from the battery. This has a negative influence on, for example, the battery cycle-life and recombination kinetics.

2.2.2. Overdischarging

Protection against overdischarging is another factor of importance, especially when NiMH batteries, which inevitably reveal small differences in storage capacities, are used in series. This implies that some batteries are already completely discharged, while others still contain small amounts of electrical energy. Continuation of the discharge process induces over discharging to occur with the already fully discharged batteries. Under these circumstances, water is forced to reduce at the Ni electrode (see Figure 5.3-2), according to:

$$2\ H_2O + 2e^- \xleftrightarrow{\text{Ni}} 2OH^- + H_2, \tag{5.3-6}$$

which also results in a pressure build-up inside the battery when no precautions are taken. This decomposition reaction takes place at rather negative potentials at the Ni electrode (i.e., more than 1.3 V more negative with respect to the Ni^{II}/Ni^{III} redox potential), as is indicated in curve (a) of Figure 5.3-7.

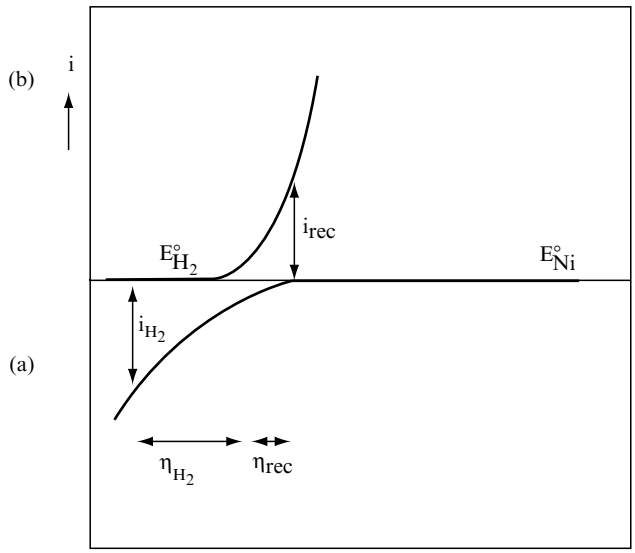

Figure 5.3-7. Schematic representation of the overdischarging process inside an NiMH battery. The hydrogen evolution reaction occurs at rather negative potentials at the Ni electrode (curve (a)), and oxidation of hydrogen occurs at the MH electrode (curve (b)) in the same potential region, resulting in a battery voltage close to 0 V.

As the (electro)chemical affinity of the MH electrode towards hydrogen gas is excellent, it is evident that this gas can be again converted into water at the MH electrode during overdischarging, according to:

$$H_2 + 2OH^- \leftrightarrow 2H_2O + 2e^-. \tag{5.3-7}$$

Whether conversion of molecular hydrogen occurs directly at the MH electrode or atomic hydrogen is oxidized indirectly after chemical adsorption and/or absorption has taken place, is not clear. It is, however, obvious that in both cases, high demands are put on the physical properties of the electrode/electrolyte interface [10]. The electrochemical oxidation also occurs close to the OH^-/H_2O redox potential (curve (b) of Figure 5.3-7). This means that the cell voltage of NiMH batteries is expected to be close to 0 V under these overdischarging conditions, or even invert to some minor extent when the overpotential contributions of both reactions are taken into account. The experimental result of such a process is shown in Figure 5.3-8, and is in agreement with these expectations. During normal discharging the battery voltage is located around 1.2 V and drops indeed towards an inverted voltage of -0.2 V when the overdischarge reactions

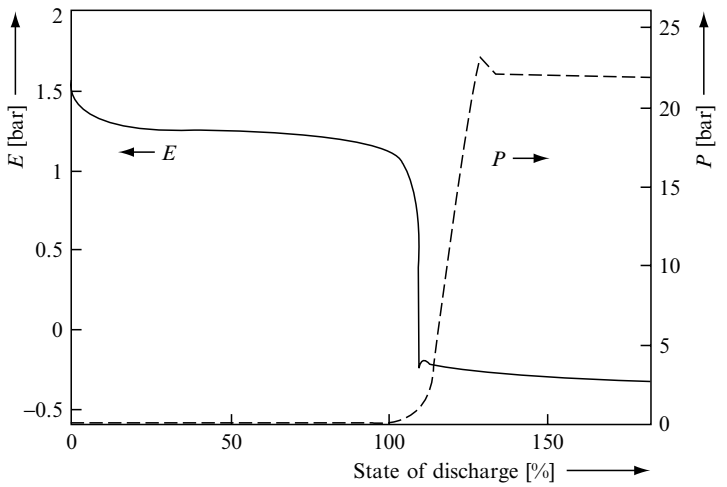

Figure 5.3-8. Experimental result of the development of the cell voltage (E) and the gas pressure (P) as a function of state-of-discharge for an NiMH battery during discharging and overdischarging.

take over. Figure 5.3-8 also reveals that the pressure rises due to hydrogen evolution may be considerable. In the example given, the pressure was quickly built up to the critical level of approximately 20 bars.

At that level the safety vent was forced to open, which can be recognized on the small pressure decrease. After a short period of time the vent closes again. Since the overpotentials of both the hydrogen evolution and hydrogen recombination reaction are relatively low during overdischarging (see Figure 5.3-7), their contribution to the heat evolution will be rather limited. This strongly contrasts to the overcharging situation described above.

In conclusion we can say that a hydrogen recombination cycle controls the pressure rise inside NiMH batteries under overdischarging conditions. As hydrogen evolution and hydrogen oxidation at the separate electrodes take place in the same potential region (see Figure 5.3-7), it is obvious that the battery voltage is very close to 0 V under these conditions. This strongly contrasts to NiCd batteries, for which a large potential reversal is generally observed during prolonged overdischarging as is shown in the subsequent section.

2.2.3. Self-discharge

It is well-known that charged NiMH batteries, similar to all rechargeable batteries, lose their stored charge under open-circuit conditions to a certain extent. The self-discharge rates are strongly dependent on external

conditions, such as, for example, the temperature of the batteries. Typical self-discharge rates at room temperature are of the order of 1% of the nominal storage capacity per day. An example of the variation in self-discharge rate for an NiMH battery as a function of temperature is shown in Figure 5.3-9.

Various mechanisms contribute to the overall self-discharge rate. These mechanisms are all electrochemical in nature. The mechanism operative in NiMH batteries occurs mainly via the gas phase, and can be divided into processes initiated by the Ni electrode or by the MH electrode. The most important mechanism contributing to the overall self-discharge rate will be treated below:

(i) Considering the redox potentials of the Ni electrode (+439 mV) and that of the competing oxygen evolution reaction (+300 mV, see Figure 5.3-3), it is obvious that trivalent Ni^{III} is thermodynamically unstable in an aqueous environment. As a consequence, NiOOH will be reduced by hydroxyl ions at the open-circuit potential, according to:

$$NiOOH + H_2O + e^- \rightarrow Ni(OH)_2 + OH^-, \tag{5.3-8}$$

$$4\ OH^- \xrightarrow{Ni} O_2 + 2H_2O + 4e^-. \tag{5.3-9}$$

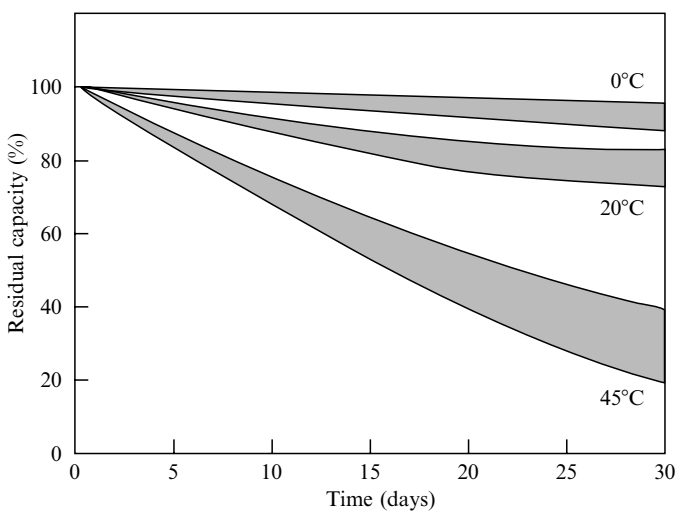

Figure 5.3-9. Dependence of the self-discharge rate on the temperature for an NiMH battery.

These reactions, occurring at the Ni electrode at a rate given by the exchange current, are represented by curves (a) and (b) in Figure 5.3-10, respectively.

The electrons released by the OH^- ions are transferred to the Ni electrode at the electrode/electrolyte interface. Although the Ni^{III} species are thus in principle unstable, electrical charge can, however, be stored in the form of chemical energy in the Ni electrode. This is due to the fact that the kinetics of the oxygen evolution reaction are, fortunately, relatively poor, so that it takes quite a while before capacity loss due to battery self-discharge becomes appreciable. Subsequently, the produced oxygen gas can be transported to the MH electrode, where it can be converted again into OH^- ions at the expense of charge stored in the MH electrode, that is,

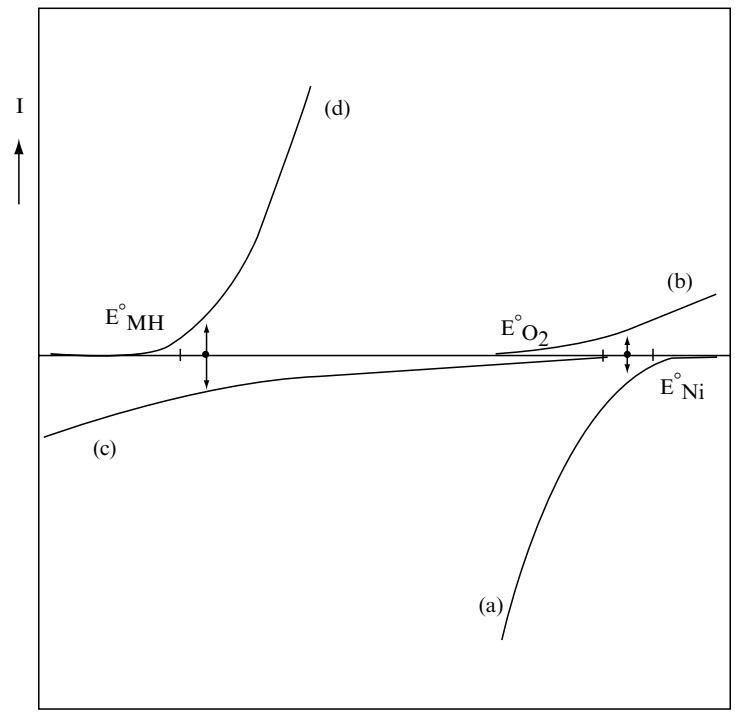

Figure 5.3-10. Schematic representation of the "oxygen gas phase shunt," partly responsible for the self-discharge behavior under open-circuit conditions of aqueous rechargeable batteries, like NiMH. Oxygen evolution (curve (a)) is initiated at the Ni electrode, which is simultaneously discharged (curve (b)) at the open-circuit potential. Consequently, O_2 can be reduced at the MH electrode (curve (c)) at the expense of electrochemically stored hydrogen (curve (d)).

$$O_2 + 2H_2O + 4e^- \xrightarrow{MH} 4OH^-, \tag{5.3-10}$$

$$MH + OH^- \rightarrow M + H_2O + e^-. \tag{5.3-11}$$

These reactions, also occurring at the open-circuit potential at the MH electrode, are represented by curves (c) and (d) in Figure 5.3-10. In the steady-state, all reaction rates are equal. Furthermore, Figure 5.3-10 indicates that the battery open-circuit voltage is around 1.2 V. The ultimate result is that charge stored in both the Ni and MH electrode is slowly released through a gas-phase shunt, in this case oxygen gas.

(ii) A different type of gas-phase shunt is initiated by the MH electrode and is caused by the presence of hydrogen gas inside the battery. As the storage capacity of the MH electrode is considerably larger than that of the Ni electrode (see battery concept in Figure 5.3-2), and the MH electrode contains a certain amount of precharge in the form of hydride, a minimum partial hydrogen pressure is inevitably established inside the NiMH battery, according to the chemical equilibrium

$$MH \leftrightarrow M + 1/2H_2 \uparrow. \tag{5.3-12}$$

The minimum H_2 pressure is dependent on the condition of the battery, but will often be determined by the hydrogen plateau pressure, which is characteristic for many hydride-forming compounds. As a result, H_2 is in contact with the Ni electrode. Since the standard redox potential of the OH^-/H_2 redox couple is much more negative than that of the Ni^{II}/Ni^{III} couple, hydrogen can be oxidized at the Ni electrode, whereas the Ni-electrode is simultaneously reduced, according to

$$H_2 + 2OH^- \xrightarrow{Ni} 2H_2O + 2e^-, \tag{5.3-13}$$

$$NiOOH + H_2O + e^- \rightarrow Ni(OH)_2 + OH^-. \tag{5.3-14}$$

Since the oxidation of hydrogen gas takes place more than 1.2 V more positive with respect to its standard redox potential and the kinetics of this reaction is very favorable, it is likely that the oxidation reaction at the Ni electrode becomes diffusion-controlled. This implies that the oxidation current, which generally reveals an exponential dependence on the voltage,

will level off to become constant at higher voltage levels. Such diffusion-controlled oxidation process, as represented by Equation (5.3-13) is schematically indicated in curve (a) of Figure 5.3-11.

The Ni reduction reaction (Equation 5.3-14) is represented by curve (b). The overall electrochemical process occurs under open-circuit conditions at the Ni electrode and will be strongly influenced by the partial hydrogen pressure inside the battery. It has indeed been reported that the self-discharge rate at the Ni electrode is proportional to the partial hydrogen pressure [10]. For this reason it is important that the hydrogen pressure inside the battery is kept as low as possible (i.e., to employ hydride-forming compounds), which are characterized by a relatively low hydrogen plateau pressure. Again, according to Equations (5.3-12) and (5.3-14), the chemical energy stored in both the MH and Ni electrode is wasted by a gas-phase shunt and can no longer be employed for useful energy supply.

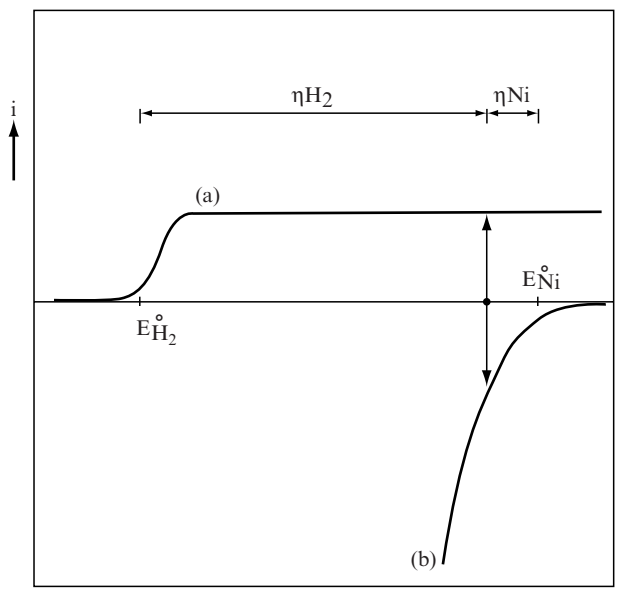

Figure 5.3-11. Schematic representation of the "hydrogen gas phase shunt," occurring during self-discharge inside an NiMH battery under open-circuit conditions. The hydride stored in the MH electrode is inevitably in equilibrium with hydrogen in the gas phase. H_2 gas can be oxidized at the Ni electrode (curve (a)) at positive potentials, where NiO_2H simultaneously is reduced (curve (c)). The oxidation current is shown to be diffusion-controlled, resulting in an anodic current plateau. It has indeed been shown that the self-discharge rate is proportional to the partial hydrogen pressure inside NiMH batteries.

(iii) The third self-discharge mechanism is related to the fabrication process of the Nickel-oxide electrode. These solid-state electrodes are generally prepared by electrolytic reduction of an acidic salt electrolyte, often $Ni(NO_3)_2$ [2]. During this process, NO_3^- ions are reduced to NH_4^+ ions. This results in a significant increase in pH near the electrode/electrolyte interface. The solubility product of $Ni(OH)_2$ will be exceeded and, as a result, $Ni(OH)_2$ will subsequently precipitate on the substrate. A consequence of this process is that, despite the fact that the as-prepared electrodes are thoroughly washed, a certain amount of nitrate ions are inevitably incorporated into the Ni electrodes, which can be leached out during the battery cycle-life. These NO_3^- ions, dissolved in the liquid phase, form the basis of this third self-discharge mechanism. These ionic species can be reduced to lower oxidation states [11]. It is generally assumed that a so-called nitrate/nitrite shuttle is operative in alkaline rechargeable batteries [12]. The standard redox potential of the nitrate/nitrite redox couple [11] is much more positive than that of the MH electrode (−91 mV versus Hg/HgO, see also Figure 5.3-3). This implies that ions delivered by the Ni electrode can be reduced at the MH electrode under open-circuit conditions, according to

$$NO_3^- + H_2O + 2e^- \xrightarrow{\text{MH}} NO_2^- + 2OH^-, \tag{5.3-15}$$

$$\mathrm{MH + OH^- \rightarrow M + H_2O + e^-}. \tag{5.3-16}$$

These reactions are schematically indicated by curves (a) and (b), respectively, in Figure 5.3-12.

The produced nitrite ions can diffuse to the Ni electrode. As the electrode potential of the Ni electrode is more positive than the redox couple of the nitrate/nitrite couple can be converted to nitrate again (curve (c) of Figure 5.3-12), while NiOOH is simultaneously reduced (curve (d)), according to

$$NO_2^- + 2OH^- \xrightarrow{\text{Ni}} NO_3^- + H_2O + 2e^-, \tag{5.3-17}$$

$$\mathrm{NiOOH + H_2O + e^- \rightarrow Ni(OH)_2 + OH^-}. \tag{5.3-18}$$

This reaction sequence can proceed continuously, as the electroactive nitrate and nitrite species are continuously produced at both electrodes. The

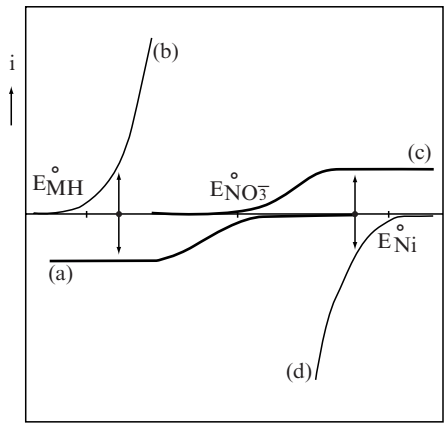

Figure 5.3-12. Schematic representation of the so-called nitrate/nitrite (NO_3^-/NO_2^-) shuttle, which takes place in the electrolyte phase. This "electrolyte shunt," induced by leaching out the Ni electrode starts with the NO_3^- reduction at the open-circuit potential of the MH electrode (curve (a)), at which the stored hydrogen simultaneously is oxidized (curve (b)). The produced NO_2^- ions are transported and converted again to NO_3^- (curve (c)) at the Ni electrode, which itself is reduced (curve (d)).

final result is again that, charge stored in both the MH and Ni electrode is consumed and no longer is available for useful energy supply.

2.2.4. NiMH charging and discharging characteristics

The most common charging method for NiMH batteries is constant current charging. The current has, however, to be limited in order to avoid an excessive rise of temperature and/or internal gas pressure (see Figure 5.3-6). This means that severe overcharging has to be terminated by a reliable end-of-charge detection. The most commonly applied method is based on a voltage drop ($-\mathrm{d}V/\mathrm{d}t$) induced by the temperature increase during overcharging. Figure 5.3-13 shows the impact of the charging current on the overall battery voltage at ambient temperature. According to kinetic considerations, the battery voltage is indeed expected to increase with increasing currents not only in the "Ni region" at low depth-of-charge (DoC), but also in the "oxygen region" at high DoC.

The transition between these two regions is somewhat dependent on the charging current in that it is shifting towards lower DoC when the current is increased, making the competition between the Ni and O_2 reaction more severe. Furthermore, it should be noted that the $-\mathrm{d}V/\mathrm{d}t$ effect is much more pronounced at higher currents, resulting from a higher heat production. This is in agreement with the relationship given in Equation (5.3-5).

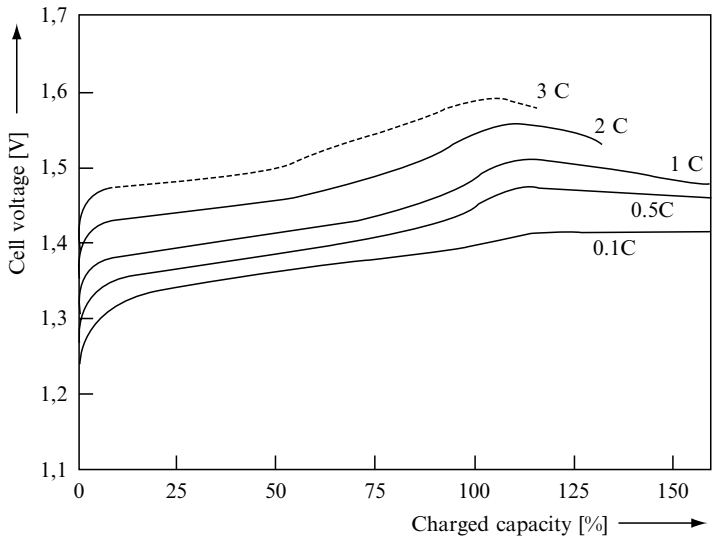

Figure 5.3-13. Cell voltage versus time during charging of NiMH batteries at 25°C at various charging rates.

The capacity of an NiMH battery depends strongly on the conditions, such as the rate of discharge and the ambient temperature. Parameters like cut-off voltage, cycle-life, and general cell condition have a minor effect. The influence of the discharge rate is shown in Figure 5.3-14.

For every battery system, energy is "lost" in two different ways during battery use. In the first place, there is a "virtual los" in discharge capacity, which is fairly limited up to currents of 1 A. The term virtual means that the capacity is not really lost, but is inaccessible at high currents due to the established concentration gradients. Secondly, further energy is lost by the drop of the discharge voltage with increasing currents, which may become very pronounced at high currents (Figure 5.3-14). This energy is really lost and is dissipated as heat (see Equation 5.3-5).

These effects are further accentuated at lower temperatures, as is depicted in Figure 5.3-15. The combination of high discharge rate and low temperature boost the virtual capacity loss. Note the increasing effect of the cut-off voltage level at higher discharge rates, particularly at low temperatures. An arbitrary cut-off voltage level of 1 V is adopted in Figure 5.3-15, and it shows that it makes quite some difference for the discharged capacity whether one discharges at 25 or 0°C, especially at a high drain current of 4 A required for (e.g., power tools).

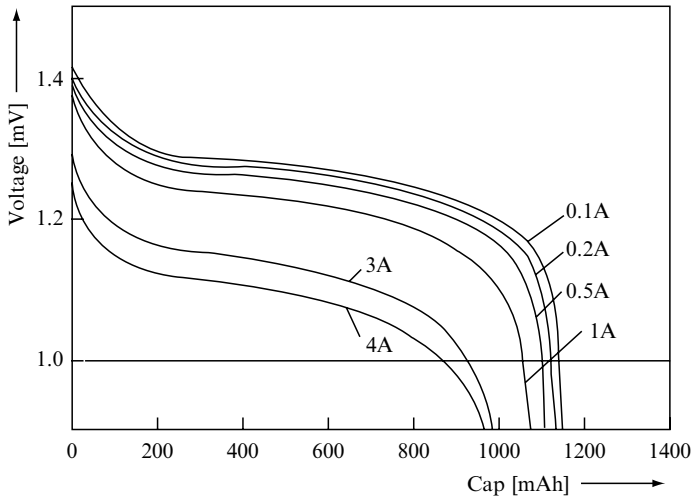

Figure 5.3-14. Influence of the discharge current on the cell voltage and discharge capacity for an AA-size NiMH at 25°C.

2.3. Nickel–Cadmium Batteries

The principles outlined in the previous section for NiMH batteries are, in several aspects, very much alike for NiCd batteries. The concept of an NiCd battery and the basic electrochemical reactions are represented in Figure 5.3-16.

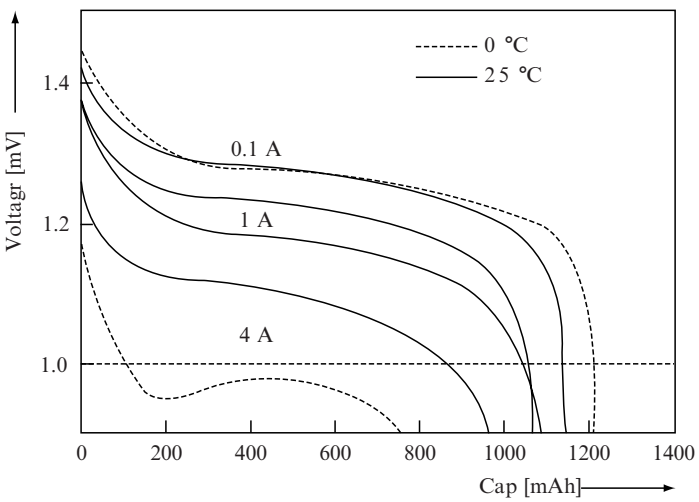

Figure 5.3-15. Influence of the discharge current on the development of the cell voltage for an AA-size NiMH battery at 0 (dashed lines) and 25°C (solid lines).

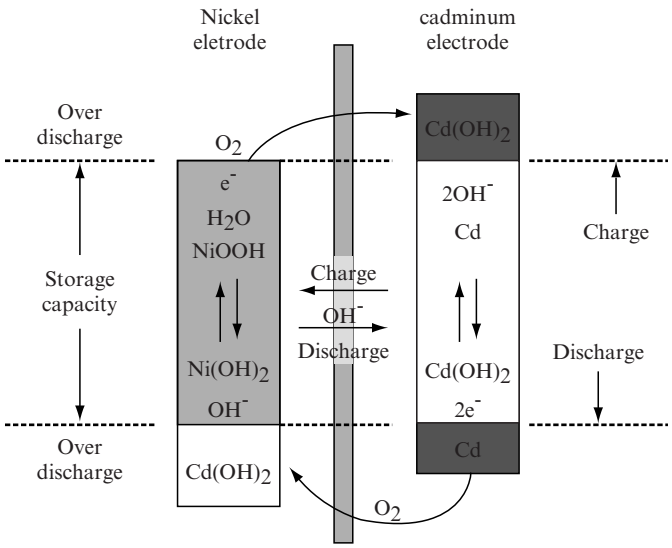

Figure 5.3-16. The concept of a sealed rechargeable NiCd battery.

Evidently, the electrochemical behavior of the nickel electrode is similar to that employed in NiMH batteries, although it should be noted that the performance may differ considerably due to relatively small variations in chemical composition. The electroactive cadmiumhydroxide ($Cd(OH)_2$) species are converted into metallic cadmium (Cd) via a complex series of intermediate chemical dissolution/precipitation reactions during charging. Since the charge transfer reaction is reversible, the opposite reaction occurs during discharging. The white areas of both electrodes represent the nominal storage capacity of the battery. The basic electrochemical charge transfer reactions in its most simplified form are as follows:

$$Ni(OH)_2 + OH^- \underset{d}{\overset{ch}{\longleftrightarrow}} NiOOH + H_2O + e^-, \qquad (5.3-19)$$

$$Cd(OH)_2 + 2e^- \underset{d}{\overset{ch}{\longleftrightarrow}} Cd + 2OH^-. \qquad (5.3-20)$$

In order to ensure the overcharge and overdischarge ability of sealed rechargeable NiCd batteries, these batteries are designed in a very specific way, which is partly based on the same concepts as explained for NiMH batteries. Especially, the gas recombination cycle initiated during over-

charging is exactly the same for NiCd and NiMH batteries. Since both systems are based on aqueous electrolytes, and since the Ni electrode is the capacity-determining electrode in these systems, it is obvious that oxygen evolution is forced to take place at the Ni electrode during overcharging. Simultaneously, reduction of $Cd(OH)_2$ in excess present in the Cd-electrode still continues according to reaction (Equation 5.3-20). As a result, the partial oxygen pressure within the cell starts to rise and induces electrochemical conversion of O_2 at the Cd-electrode. The same reaction sequence takes place, as represented by Equations (5.3-3) and (5.3-4), and was illustrated in Figure 5.3-5. As both reactions also occur at very similar electrode potentials during overcharging (i.e., at relatively high overpotentials), the temperature development is expected to be very similar to that of NiMH batteries. Dependent on the competition between reactions in Equations (5.3-20) and (5.3-4), the gas pressure and/or the temperature of the battery will rise during overcharging. Figure 5.3-17 indeed shows that both the development of the internal gas pressure and temperature increases at the end of the charging process where the overcharging reactions start to proceed.

Differences between these characteristics may be due to differences in reaction kinetics and also to different charging conditions, such as overcharging current. The potential decrease ($-dV/dt$), for example, is generally more pronounced for NiCd than for NiMH, which makes an end-of-charge detection based on this phenomenon easier for NiCd batteries than for NiMH batteries.

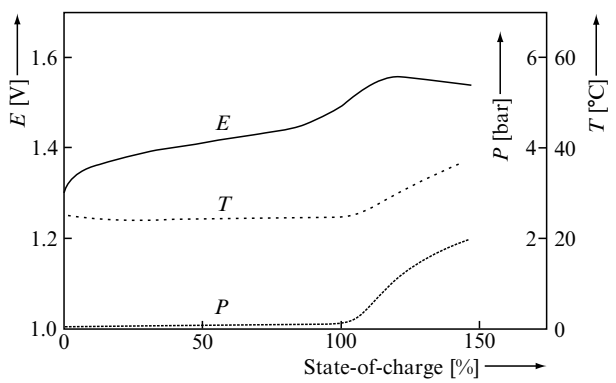

Figure 5.3-17. Development of the cell voltage (E), the internal gas pressure (P), and the battery temperature (T) of an NiCd battery as a function of state-of-charge during charging with a current of 0.6 A (1 C-rate). Clearly, overcharging has quite a different impact on these parameters than the normal charging process.

Protection against overdischarging NiCd batteries is somewhat more complex for NiCd than for NiMH batteries. Since a hydrogen recombination cycle has to be avoided due to the poor electrocatalytic activity of the Cd-electrode with respect to the H_2 oxidation reaction, battery manufacturers adopted another elegant approach. A significant amount of $Cd(OH)_2$, generally denoted as depolarizer, is added to the Ni-electrode and, to a lesser extent, some metallic Cd is added to the Cd-electrode as discharge reserve (see shaded overdischarge areas in Figure 5.3-16). During overdischarge, the $Cd(OH)_2$ present in the Ni-electrode is reduced to metallic Cd (Equation 5.3-20), while the excess of metallic Cd is still being oxidized at the Cd-electrode. As the amount of extra Cd with respect to $Cd(OH)_2$ is limited, oxygen gas will be evolved at the Cd-electrode during continuation of the discharge process. Again an oxygen recombination cycle is established, now starting at the cadmium electrode, as is indicated in Figure 5.3-16.

The theoretically expected development of the electrode potential of the Ni (curve (a)) and the Cd-electrode (curve (b)) during both the discharge and overdischarge process are shown in Figure 5.3-18.

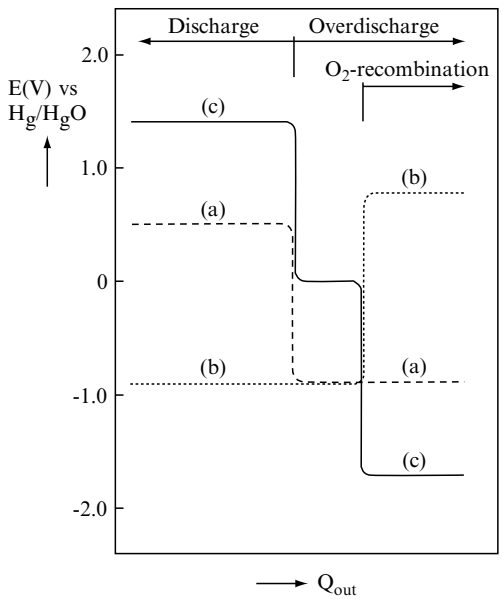

Figure 5.3-18. Schematic representation of the potential dependence of an NiCd battery during discharging and overdischarging. The potentials of the separate Ni and Cd electrodes are represented by the dashed curves (a) and (b), respectively, and are given with respect to an Hg/HgO reference electrode. The development of the total cell voltage is shown by the solid line (curve (c)). The two stages of the overdischarge process can clearly be recognized.

The two different stages, characteristic for the overdischarge process, can clearly be recognized in this figure and have a pronounced influence on the total cell voltage ($E_{Ni} - E_{Cd}$), as is schematically shown in curve (c) of Figure 5.3-18. During the first stage of overdischarging, the same redox reaction takes place at both electrodes and a cell voltage close to 0 V is therefore to be expected. When the oxygen recombination cycle starts (i.e., when O_2 is evolved at the Cd-electrode at positive potentials (curve (b) of Figure 5.3-18)), and converted again into OH^- at the Ni-electrode at very negative potentials (curve (a)), a potential reversal of the battery is indeed to be expected (curve (c)).

An experimental result of such overdischarge process is shown in Figure 5.3-19. The potential dependence is very much the same as for the predicted potential. Once the NiCd battery is fully discharged, electrochemical transition of Cd-species occurs at both electrodes and, consequently, the cell voltage is close to 0 V at the first overdischarge plateau. Evidently, as the overpotential contributions of both electrochemical reactions are very limited, the heat production is relatively small. This results in a very limited temperature increase in this first plateau region (see T-curve in Figure 5.3-19). Continuation of overdischarging leads to cell potential reversal; a second potential plateau, in this case around -1.8 V, is established, at which the oxygen recombination takes place. In agreement with the theoretical considerations given above, the temperature rise is here much more pronounced and is very similar to that under

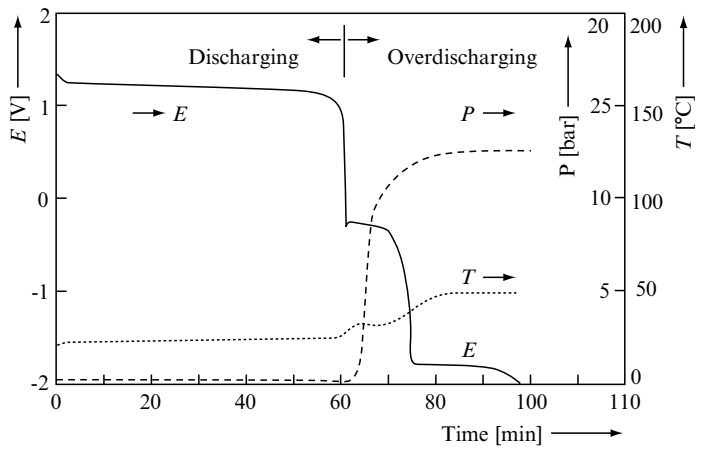

Figure 5.3-19. The characteristic response of the cell voltage (E), internal gas pressure (P), and temperature (T) of an NiCd battery during (over)discharging with a current of 1.2 A (2 C-rate).

overcharge conditions. Although the processes occurring during overcharging and overdischarging are essentially the same, the kinetics of these processes need not necessarily be the same. This becomes clear when one considers the pressure build-up during both processes. The experimental results generally reveal that the pressure during overdischarging rises more rapidly than during overcharging, indicating that the oxygen recombination kinetics at the Cd electrode is more favorable than at the Ni electrode. This sometimes results in a very steep pressure increase, as is shown by the P-curve in Figure 5.3-19.

The well-known memory effect is related to the complex dissolution/precipitation mechanism of the Cd electrode. As has been pointed out, the Cd electrode is composed of a two-phase morphology and the crystallite sizes determine the kinetics of these electrodes. Under normal operation conditions, these crystallite sizes will be small and, consequently, the surface area reasonably high. When the Cd electrode is operated under these normal conditions, the current density will be relatively low for the entire electrode. On the other hand, when only a small part of the storage capacity is frequently used, that part, which is not under continuous current flowing conditions, are allowed to recrystallize. As a result, those effectively ''unused'' electrode parts recrystallize into much larger morphological structures, which results in a much lower surface area. When at a certain moment, this part of the electrode is charged and/or discharged, the current density and consequently the overpotentials will be much larger than for those parts, which were frequently under (de)loading conditions. This results in a virtual capacity loss. This virtual capacity loss can be diminished by charging and discharging the battery over the entire capacity for a few cycles.

Some discharging characteristics for NiCd are shown in Figure 5.3-20. Similar trends as for NiMH (Figure 5.3-14) can be seen: (1) the voltage drops when the current is increased due to the inevitable overpotential losses and (2) a virtual capacity loss is observed as transport limitations are playing a more dominant role at higher currents. As discussed before, this is not a real capacity loss, as all capacity can be discharged when the system is allowed to equilibrate so that the built-up concentration gradients can be minimized again.

2.4. Li–Ion Batteries

So far, this contribution has been restricted to aqueous rechargeable battery systems. The battery voltage of these systems is dominated by the decomposition potentials of water. In this section, we concentrate on a non-aqueous and relatively new system, which has reached its mature

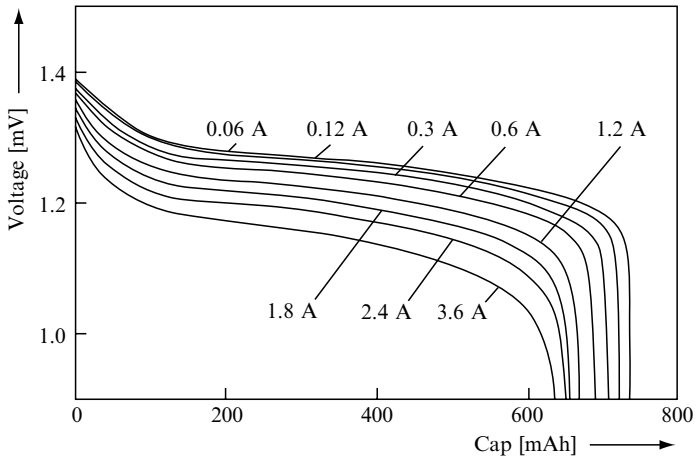

Figure 5.3-20. Development of the cell voltage of an AA-size NiCd battery at 25°C and various discharge currents.

commercialization stage for one decade now: the lithium–ion battery. This battery type differs from aqueous systems in several aspects. In the first place, lithium is a base metal having a very negative value for the standard redox potential (less than −2.5 V versus Hg/HgO; compare with values indicated in Figure 5.3-3). Combining an electrode based on this redox system with a second electrode having a positive redox potential leads to a battery concept with an extremely high cell voltage, of the order of 3.5 up to 4.0 V. In the second place, the molecular weight of some lithium and some lithium-host materials are relatively low, which may result in battery systems with potentially high energy densities, as was already mentioned in relation to Table 5.3-1. In order to make use of lithium as negative electrode material, water and air have, however, to be excluded. Aqueous electrolyte solutions can therefore not be employed, as Li is unstable in this environment. Consequently, all lithium systems are based on organic electrolytes, either in the liquid or the solid form. Conventional Li–ion batteries are nowadays exclusively based on liquid organic electrolytes. All-solid-state Li–ion batteries will become more important in the near future for smaller applications in the field of *Autonomous devices* in the context of *AmI*. But the basic principles apply for both systems.

The concept of a rechargeable Li–ion battery is relatively simple and is shown in Figure 5.3-21.

The positive electrode generally consists of trivalent cobaltoxide species, in which lithium ions are intercalated ($LiCo^{III}O_2$). During charging, trivalent $LiCoO_2$ is oxidized into four-valent $Li_{1-x}Co^{IV}O_2$ and the excess

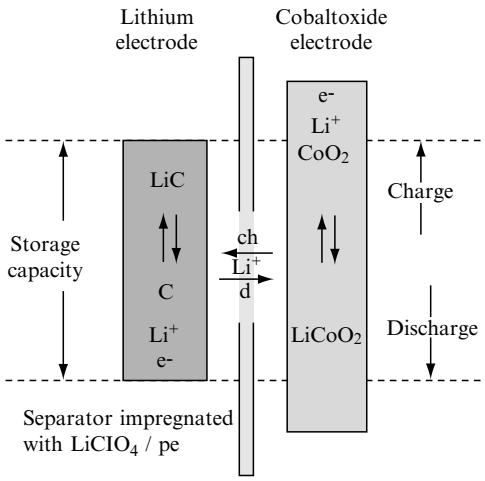

Figure 5.3-21. Concept of a sealed rechargeable Li–ion battery.

of positive charge is liberated from the electrode in the form of Li ions, according to

$$\mathrm{LiCo^{III}O_2} \underset{d}{\overset{ch}{\longleftrightarrow}} \mathrm{Li_{1-x}Co^{IV}O_2} + \mathrm{xLi^+} + \mathrm{xe^-}. \qquad (5.3-21)$$

The Li^+ ions dissolve into the electrolyte. For a proper reversible functioning of a Li–ion cell, not all Li^+ ions can be removed from the solid. This implies that x can, in practice, not become lower than 0.45. The electrolyte generally consists of an organic solution, like propylenecarbonate (PC), containing a high concentration of an Li salt (e.g., $LiClO_4$, $LiAsF_6$, or $LiPF_6$) to ensure the electrolytic conductivity between the two electrodes. Arriving at the negative electrode, Li^+ ions can be reduced. This would result in metallic lithium. It was, however, found that the formation of metallic Li unfortunately results in a poor cycle-life. Furthermore, it was recognized that the risk of dendrite formation at the Li electrode surface and, consequently, the risk of short-circuiting resulted in an unsafe design. In order to circumvent these problems, the following electrode construction has been proposed: the Li ions are transported inside a carbon (C_6) electrode and are subsequently reduced according to

$$\mathrm{Li_yC_{6d}} + \mathrm{xLi^+} + \mathrm{xe^-} \underset{d}{\overset{ch}{\longleftrightarrow}} \mathrm{Li_{y+x}C_6}, \qquad (5.3-22)$$

where the value for y, which may range from 0 to 0.7 is dependent on the nature of the used graphite. From the overall reaction;

$$LiCoO_2 + Li_yC_6 \underset{d}{\overset{ch}{\longleftrightarrow}} Li_{1-x}CoO_2 + Li_{y+x}C_6, \qquad (5.3-23)$$

it is clear that the essence is that lithium ions are transported from one electrode through the organic electrolyte to the other electrode. This basic principle is obviously very similar to that of the NiMH battery except that Lithium is involved instead of hydrogen. This transportation concept has often been denoted in speaking terms, like the ''rocking chair'' model or the ''swing'' concept to illustrate the swinging movements of the Li-ions. The advantage of this concept is that lithium is safely stored within both electrodes. A disadvantage is, of course, that the energy density has been reduced significantly with respect to potentially possible values. Inspection of Table 5.3-1 reveals that the energy density per volume is hardly higher with respect to that of, for example, the NiMH battery. The advantage can be found in the energy density per weight (Table 5.3-1). It should, however, be noted that this characteristic is often not of major importance in many electronic applications.

One of the remaining problems of Li–ion is that a thorough (electro)-chemical protection against both overcharging and overdischarging is not (yet) available. Recombination cycles, as employed in NiMH and NiCd batteries, do not exist at the moment for Li–ion batteries. However, it should be emphasized that the organic electrolyte can also be decomposed, whereas recombination of the decomposition products into the original organic solvent has not been realized yet. This implies that overcharging and overdischarging has to be avoided under all circumstances, and care should be taken that the cell potential is never outside the potential range in which the basic electrochemical reactions occur. An excellent method to accomplish this is, charging and discharging at a constant potential until the voltage limits are reached. An example of a typical constant-current-constant-voltage (CCCV) charging profile is shown in Figure 5.3-22 reveals the development of the cell voltage (E), the applied current (I), and the stored capacity. In the initial stage, the battery is charged rapidly with a moderate constant current.

The maximum height of the current is, for safety reasons, generally prescribed by the battery manufacturer. Figure 5.3-22 shows that the cell voltage is gradually increased up to a value of 4.2 V. This value is considered to be the upper allowable limit and ensures a proper functioning of the battery. As soon as this limit is reached, the charging regime changes from amperostatic (CC) to potentiostatic (CV-mode). As a result the current is adapted in this region and decreases rapidly to lower values.

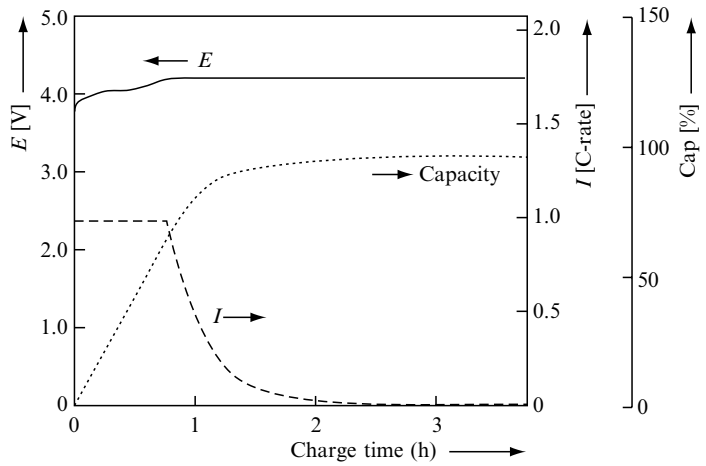

Figure 5.3-22. Constant -current-constant-voltage (CCCV) charging regime typical for Li–ion batteries.

Evidently, charging proceeds more slowly which can be recognized by the inhibited increase of the storage capacity. At the end of the charging process, the current diminishes to very low values when the battery is fully charged. In total charging takes more than 1 hour. Recently, we have proposed the concept of boostcharging in order to cope with the customer request to more quick charge Li–ion without introducing any negative cycle-life effects [13]. In this way, for example, one third of its rated capacity can be charged within 5 min [13].

Some discharge characteristics as a function of the current level are shown in Figure 5.3-23. Again, the same two trends are observed. Firstly, due to larger overpotentials the voltage drops at higher currents, and secondly, the virtual capacity goes down rapidly due to transport limitations. In general, the kinetics of Li–ion is somewhat poorer compared to those of NiCd and NiMH.

The self-discharge rates of commercially available Li–ion batteries are, on the other hand, generally somewhat lower than that of the aqueous systems. Although the self-discharge mechanism is not fully understood, it is likely that the origin must also be sought in the electrochemical instability of the organic electrolyte. The specified self-discharge rates are nowadays of the order of 0.1% per day at room temperature. Following the reasoning of the previous two sections, it is clear that the large temperature increase found for the aqueous systems during overcharging is not observed for Li–ion batteries, because a corresponding recombination cycle does not exist.

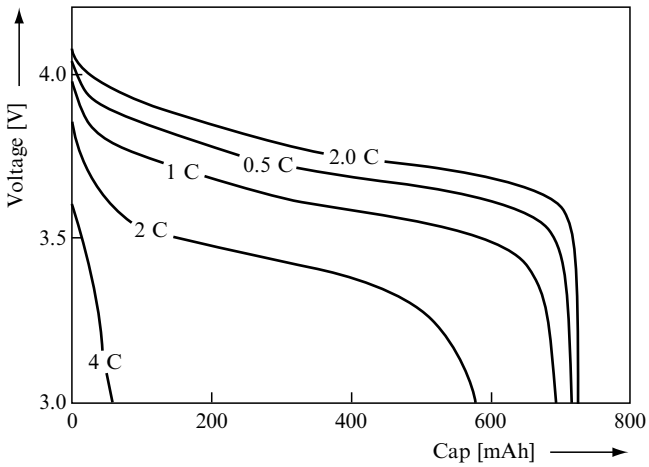

Figure 5.3-23. Development of the discharge voltage of a cylindrical Li–ion battery at 25°C at various discharge rates.

REFERENCES

[1] Linden, D. (ed), 1995, *Handbook of Batteries*, 2nd edition, McGraw-Hill, New York.
[2] Notten, P. H. L., 1994, Rechargeable Nickel-Metalhydride Batteries: A Successful New Concept, Chapter 7, *in* Grandjean, et al. (eds), *NATO ASI Series E*, Volume 281, London.
[3] Notten, P. H. L. and van Beek, J. R. G., 2000, *Chem. Ind.*, **54,** 102–115.
[4] Kruijt, W. S., Notten, P. H. L. and Bergveld, H. J., 1998, *J. Electrochem. Soc.,* **145,** 3764.
[5] Notten, P. H. L., Kruijt, W. S. and Bergveld, H. J., 1998, *J. Electrochem. Soc*., **145,** 3774.
[6] Bergveld, H. J., Notten, P. H. L. and Kruijt, W. S., 1999, *J. Power Sources*, **77,** 143.
[7] Ledovskikh, A., Verbitskiy, E., Ayeb, A. and Notten, P. H. L., 2003, *J. Alloys Comp*., **742,** 356–357.
[8] Bergveld, H. J., Kruijt, W. S. and Notten, P. H. L., 2002, *Battery Management Systems: Design by Modelling*, Kluwer Academic Publishers.
[9] Notten, P. H. L., Verbitskiy, E., Kruijt, W. S. and Bergveld, H. J., *J. Electrochem. Soc*., **152** (2005) A 1423.
[10] Kim, Y. J., Vinsintin, A., Srinivasan, S. and Appleby, A. J., 1992, *J. Electrochem. Soc*., **139,** 351.
[11] Bard, A. J., Parsons, R. and Jordan, J. (eds), 1985, *Standard Redox Potentials in Aqueous Solutions*, Marcel Dekker, New York.
[12] Kohler, U. and Dekker, Ch., 1993, *Dechema Monochraphien,* **128,** 213.
[13] Notten, P. H. L., van Beek, J. R. and Op het Veld, J. H. G., *J. Power Sources*, **145,** 89, 2005.